processes

MDPI

Article

Carbon Dioxide Prevents Oxygen Adsorption at Low-Temperature Oxidation Stage of Low-Rank Coal: Laboratory Study and Molecular Simulation

Gang Cheng [1,2,*], Haiyan Wang [3,*], Bo Tan [2] and Shuhui Fu [2]

[1] School of Geology and Mining Engineering, Xinjiang University, Urumqi 830047, China
[2] School of Emergency Management and Safety Engineering, China University of Mining and Technology (Beijing), Beijing 100083, China; tanbo709@126.com (B.T.); wy19800302517@163.com (S.F.)
[3] School of Civil and Resource Engineering, University of Science and Technology Beijing, Beijing 100083, China
* Correspondence: gang-ch@xju.edu.cn (G.C.); whycumtb@163.com (H.W.)

Abstract: Carbon dioxide (CO_2) is widely used in the prevention and control of spontaneous coal combustion. In this manuscript, three low-rank coals with different metamorphic degrees were selected as the research objects. The temperature-programmed experiments, in situ infrared cooling experiments, simulation of the competitive adsorption of CO_2 and oxygen (O_2) in coal pores, and simulation study of the CO_2 inhibition of the coal oxygen composite reaction were used to obtain the role and effect of CO_2 in preventing oxygen adsorption in coal at the low-temperature oxidation stage. It was concluded that CO_2 can displace the O_2 near the pore wall to physically prevent the adsorption of O_2. Through the changing law of heating rate and a kinetics analysis, it was found that CO_2 can increase its activation energy by 5.3–108.3% during the slow heating stage of coal and reduce its heat rate. At around 120 °C, coal loses the protective effect of CO_2. From the changes in functional groups, it can be seen that when coal was cooled in the CO_2 atmosphere, mainly pyrolysis and condensation reactions occurred due to the lack of O_2. In addition, CO_2 can also inhibit the chain reaction of the chemical adsorption of oxygen in coal. This work provides a theoretical basis for CO_2 prevention and the control of spontaneous coal combustion.

Keywords: carbon dioxide; prevent oxygen adsorption; fire prevention and extinguishing; activation energy; heat release; competitive adsorption

Citation: Cheng, G.; Wang, H.; Tan, B.; Fu, S. Carbon Dioxide Prevents Oxygen Adsorption at Low-Temperature Oxidation Stage of Low-Rank Coal: Laboratory Study and Molecular Simulation. *Processes* **2023**, *11*, 2504. https://doi.org/10.3390/pr11082504

Academic Editor: Jan Zawała

Received: 8 July 2023
Revised: 8 August 2023
Accepted: 17 August 2023
Published: 20 August 2023

1. Introduction

Spontaneous coal combustion is one of the five major disasters in coal mines [1–3], which restricts the safe and efficient exploitation and utilization of coal resources in our country [4–6]. With the continuous in-depth research on the mechanism of spontaneous coal combustion having been conducted for a long time, scholars have proposed various theories from different angles to explain the spontaneous coal combustion phenomenon, among which the coal–oxygen composite theory [7–11] has been widely recognized. At the microscopic level, coal is viewed as a porous media material. The coal–oxygen recombination reaction at the gas–solid interface inside the medium first requires the physical adsorption of oxygen by means of intermolecular forces (van der Waals forces). Based on this, the inert gas injection fire-fighting method, which can reduce the O_2 concentration in the goaf, has been widely used in the process of spontaneous coal combustion fire control [12,13].

Among them, nitrogen (N_2) and CO_2 are widely used due to their advantages of inserting, cooling, explosion suppression, large diffusion range, no damage to instruments and equipment, and the ability to bypass obstacles [14]. At the same time, many scholars have conducted a lot of research on the effect of inert gas on preventing spontaneous combustion

of coal. Most of the research focuses on comparing the oxidation characteristics [15–20], ignition characteristics [21], combustion characteristics [22], changes in functional groups [23], and the generation of index gases [24] of coal samples in O_2/N_2 and O_2/CO_2 atmospheres. These results show that the presence of N_2 and CO_2 is helpful to prevent CSC, and the effect of CO_2 injection is better than that of N_2. However, the timeliness of the CO_2 protection of coal to prevent its spontaneous combustion is not described. Therefore, it is necessary to further clarify the mechanism of CO_2 fire prevention in order to better prevent and control spontaneous coal combustion.

In explaining the mechanism of CO_2 fire prevention, predecessors have mostly studied the adsorption and desorption mechanism of the gas. Many scholars have used the Grand Canonical Monte Carlo method to study the competitive adsorption mechanism of multiple gases using the coal unit cell model. Wu et al. [25] revealed the competitive adsorption mechanism of $CO_2/O_2/N_2$ in coal through the Grand Canonical Monte Carlo method (GCMC) and molecular dynamics (MD) simulations, indicating that CO_2 occupies a stronger adsorption site and has a stronger interaction energy with coal, so it is more easily adsorbed in coal. Zhang et al. [26] used the GCMC simulation method and concluded that the adsorption capacity of gas in lignite is greater than that of O_2 for both single and binary components. Long et al. [27] studied the adsorption and diffusion characteristics of CO_2 and N_2 in the micropore and mesopore of coal by means of molecular dynamics. Dong et al. [28] used an adsorption simulation method to reveal the adsorption properties of two kinds of bituminous coals for CO, CO_2, and O_2 at different pressures and temperatures. CO_2 is more easily adsorbed than O_2. Liu et al. [29] combined thermogravimetric analysis with the adsorption–desorption mechanism and confirmed that CO_2 and H_2O chemisorption occurred using non-isothermal experiments. Liu et al. [30] simulated the gas transport law and explored the O_2 distribution under the condition of inert gas injection into the goaf.

Coal is an extremely heterogeneous substance with abundant pores and a complex chemical structure [31,32]. The coal pore structure plays a crucial role in the process of gas adsorption, migration, and generation [33]. The above studies either did not consider the influence of pore structure, or they considered the pore structure but mostly used graphene slit pore and carbon nanotube models to simulate the nanopore structure of coal with different pore sizes. Although the above methods can effectively simplify the calculation, the coal surface has complex chemical heterogeneity and contains various functional groups, which cannot reflect the actual situation. Some scholars have confirmed that functional groups have an important influence on the adsorption of gases. Most of the above studies explain the mechanism of CO_2 fire prevention and extinguishing from the perspective of gas competitive adsorption. In addition to the above physical effects, CO_2 also has the effect of inhibiting the coal–oxygen composite chain reaction, and it is necessary to further reveal its inhibiting oxygen adsorption mechanism from a chemical point of view. The pore structure and surface chemical groups of porous materials, in particular, have a considerable impact on their adsorption and separation properties [34,35]. Moreover, the adsorption of CO_2 by the porous materials could be significantly influenced by both heteroatom and microporous porosity [36].

We innovatively used the macromolecular model of low-rank coal to construct the pore structure of coal, revealing the microscopic mechanism of gas displacement more realistically. This manuscript also creatively simulates the effect of CO_2 on the coal–oxygen complex chain reaction, and has experiments to verify it, as shown in Figure 1. This work explains both the physical and chemical effects of CO_2 in preventing oxygen adsorption. The aging time and mechanism of preventing oxygen adsorption was clarified, and a model of CO_2 preventing oxygen adsorption was constructed, which provided a theoretical basis for inert fire prevention and extinguishing.

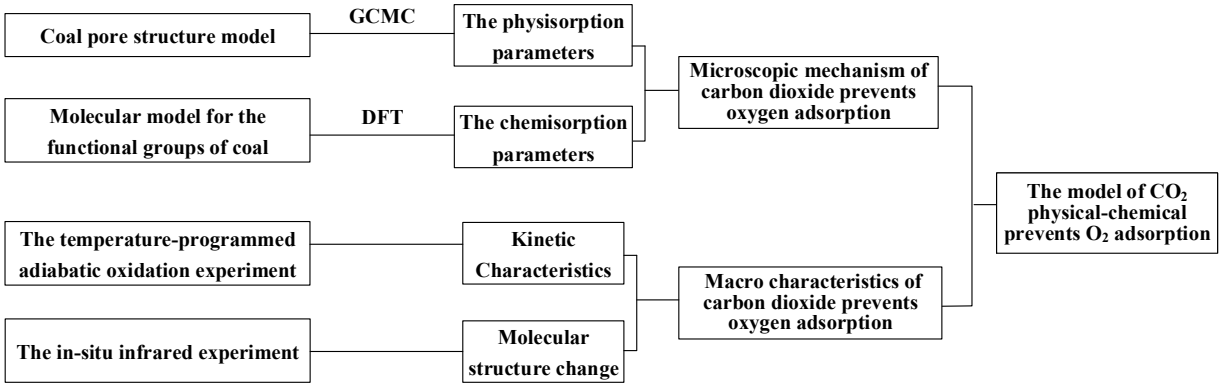

Figure 1. Molecular simulations and experimental structural diagram.

2. Coal Samples and Methods

2.1. Experimental

2.1.1. Low-Rank Coal Sample Preparation

Low-rank coal has a high propensity for spontaneous combustion in goaf or coal seams, so it is the main research object of measures to prevent spontaneous coal combustion. Therefore, this manuscript selected lignite from the Huolinhe mining area, long-flame coal from the Yuheng mining area, and gas coal from the Aiweiergou mining area as the research objects, denoted as HL, YH, and AW, respectively [37]. The low-rank coal samples were crushed into 120-mesh-pulverized coal for industrial analysis, organic element (C, H, O, N) content determination, S element content determination, and vitrinite reflectance analysis. The analysis results are shown in Table 1.

Table 1. Each low-rank coal sample's analysis results.

Coal Sample	M_{ad}	A_d	V_{daf}	FC_{ad}	C_{daf}	H_{daf}	N_{daf}	O_{daf}	$S_{t,ad}$ /%	$R_{o,ran}$ /%
HL	14.35	6.92	42.46	36.27	73.29	5.16	1.06	19.22	1.27	0.35
YH	4.67	6.18	38.09	51.06	81.92	5.24	0.93	9.32	2.68	0.58
AW	0.82	8.73	35.82	54.63	86.25	5.91	1.13	6.37	0.34	0.78

Notes: M_{ad}—moisture; A_d—ash; V_{daf}—volatile; FC_{ad}—fixed carbon; C_{daf}—carbon content; H_{daf}—hydrogen content; N_{daf}—nitrogen content; O_{daf}—oxygen content; $S_{t,ad}$—sulfur content; $R_{o,ran}$—vitrinite reflectance.

2.1.2. Device and Process of Temperature-Programmed Adiabatic Oxidation Experiment

Under the same conditions as the coal type, particle size, air flow rate, heating rate, initial temperature, and final temperature, two spontaneous coal combustion adiabatic oxidation temperature programming tests were carried out for each coal sample, as shown in Figure 2. That is, under the condition of 30 °C, air or CO_2 was respectively introduced into the coal sample with a weight of 200 g and a diameter of about 1.5–2.4 mm, and the temperature-programmed adiabatic oxidation experiment was started after holding for 2 h. The temperature was raised to 200 °C with a heating rate of 1 K/min and then held at a constant temperature for 5 h.

2.1.3. Device and Process of In Situ Infrared Cooling Experiment

The experimental test system was a TENSOR27 Fourier transform infrared spectrometer from BLUKE, Germany, which realized the testing of the changes in functional groups of coal at different temperatures through an in situ infrared reaction cell measurement. The in situ infrared reaction cell body was mainly made of 316 L stainless steel (high temperature resistance of 500 °C, pressure resistance of 3 MPa) and the reaction cell cavity cap had three windows (two infrared windows, one quartz window), providing three inlets/outlets for pumping out of the cell body and introducing gases. The general experimental program

was that coal samples (200 mesh) of about 5 g were selected each time and inserted in nitrogen for 6 h before being placed in the reaction cell. The coal samples were raised to 200 °C in an atmosphere of air (80% N_2 and 20% O_2) and then cooled down by passing CO_2 and air, respectively. The atmosphere flow rate was 50 mL/min, the resolution of the infrared test program was 4 cm^{-1}, the spectral scanning range was 800~4000 cm^{-1}, data were collected every 30 s, and the collection time was 20 to 25 min.

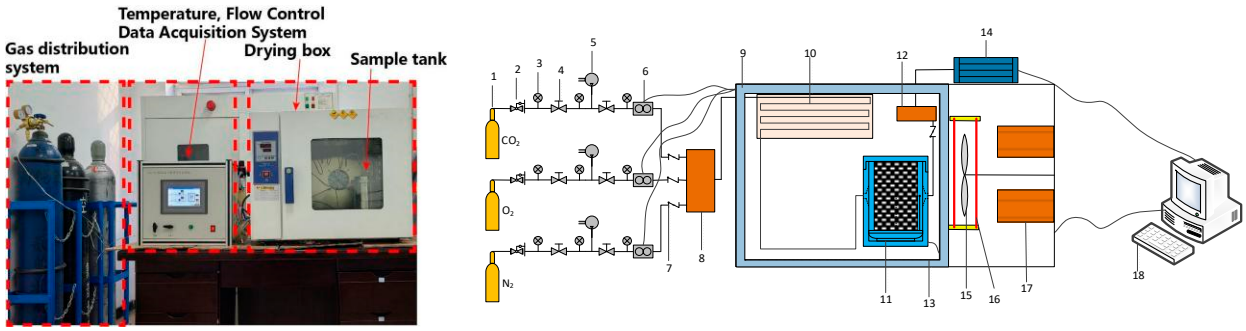

Figure 2. Experimental setup for programmed thermal adiabatic oxidation. Legend: 1—gas cylinder; 2—pressure-reducing valve; 3—pressure gauge; 4—pressure regulator valve; 5—air compressor; 6—flow meter; 7—check valve; 8—intake mixing bin; 9—insulation layer; 10—gas-preheating copper pipe; 11—heat transfer coal sample tank; 12—outlet gas-mixing chamber; 13—program temperature control box; 14—cooler; 15—fan; 16—heater; 17—refrigerator; 18—PC.

2.2. Simulation Method

The simulation methods in this paper are categorized into physical and chemical adsorption. The physisorption was mainly simulated by material studio 8.0 software based on the GCMC for competitive physisorption. Chemisorption was mainly simulated thermodynamically and kinetically by Gaussian09 software, based on the density functional method (DFT).

2.2.1. Method of Physisorption Simulation

(1) GCMC physisorption method

The physisorption simulations were carried out by the GCMC method, with the coal molecular unit cells as the adsorbent and oxygen molecules as the adsorbate [38], and the Metropolis algorithm was used to keep the chemical potential and volume stable during the simulations. The temperature was set to 298 K, the Ewald was used for the summation of electrostatic interactions and the Atom for van der Waals interactions, with the cut-off distance set to 15.5 Å.

The effect of carbon dioxide on oxygen adsorption in the coal pore structure was analyzed in the Forcite module of Materials Studio 8.0 software. The task was set to dynamics, the NVT ensemble was used, and based on the structural optimization of the initial configuration of the physisorption configurations, the molecular dynamics simulations were carried out at 298 K, a step size of 1 fs, a dynamics simulation time of 100 ps, and with the temperature control method set to Nose.

(2) Simulation of Competitive Adsorption of CO_2 and O_2 in Coal Surface Pores

The molecular structure of the HL coal sample selected for the physisorption simulation and the method of constructing the molecular pore structure of the HL coal sample can be referenced from the papers published by our group [37,39]. As shown in Figure 3, HL coal molecules were used as pore walls to construct pores with a diameter of 20 Å and a length of 155 Å. The left side of Figure 3 is the graphene structure "piston". Under the conditions of 30 °C, 60 °C, 90 °C, and 120 °C, the "piston" moved 1 Å per 100 ps to push the mixture of CO_2 and O_2 to the intake side. The length of the intake side was set to 85 Å, and

the piston pushed forward a total of 75 Å. The mixed gas consisted of 747 CO_2 molecules and 747 O_2 molecules. The height and width of the entire model were 55 Å.

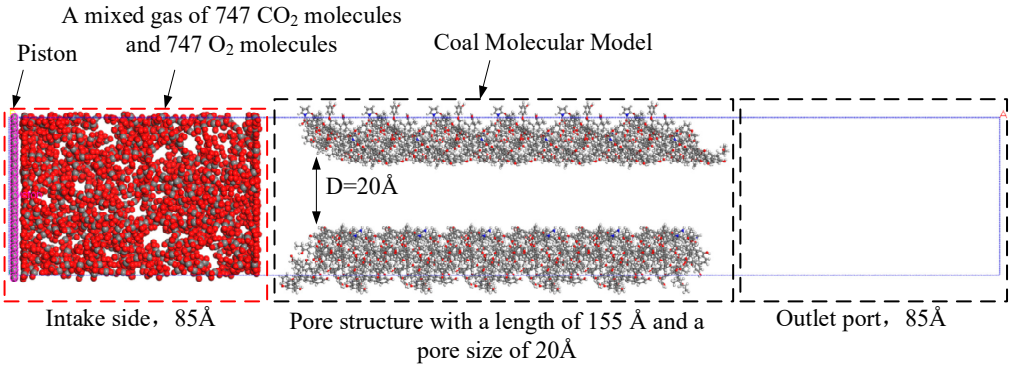

Figure 3. Gas adsorption model of coal surface pore.

2.2.2. Method for Chemisorption Simulation

In this study, calculations were performed using density functional theory (DFT), the Gaussian09 package and the M06-2x/6-31G(d,p) [40] method. For the structure optimization and frequency calculation of the reactants, the TS (Berny) method [41] was used to find the transition state, and the intrinsic reaction coordinate (IRC) method based on the LQA algorithm was used to analyze the reaction pathway. It should be noted that for groups (radicals and oxygen) with a spin multiplicity other than 1, calculations were performed in an open-shell environment.

3. Results and Analysis

3.1. Analysis on the Physical Mechanism of CO_2 Preventing O_2 Adsorption

It can be seen from the author's previous work that the adsorption capacity of CO_2 in coal is stronger than that of O_2, and CO_2 can displace O_2 in coal [38]. The mechanism of this macroscopic phenomenon is unknown, so this study used Materials Studio 8.0 software to simulate this phenomenon to explain its cause from a microscopic perspective. According to the simulation results in Materials Studio 8.0, the adsorption and diffusion of O_2 and CO_2 in the coal pore structure in each time period can be known, as shown in Figure 4.

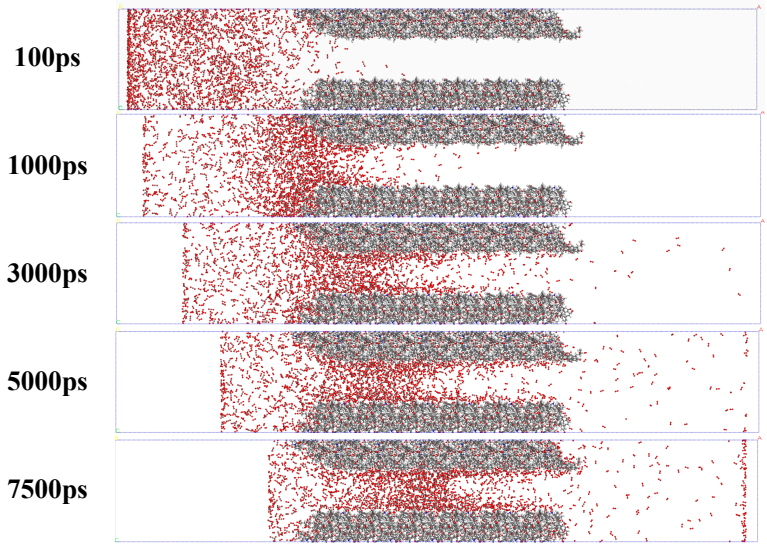

Figure 4. Adsorption and diffusion of O_2 and CO_2 in coal pore structure at 30 °C. The red dots are oxygen atomic, the black dots are carbon atomic.

Figure 5 shows the time-dependent changes in O_2 and CO_2 at the gas outlet port of the coal surface pore model at different temperatures. Under the same conditions, the amount of CO_2 at the gas outlet port is always less than the amount of O_2. At 30 °C, 60 °C, 90 °C, and 120 °C, O_2 appeared at the gas outlet port at 1500 ps, 1000 ps, 500 ps, and 100 ps, respectively, while CO_2 appeared at 2500 ps, 1500 ps, 500 ps, and 100 ps, respectively. It can be seen that O_2 can be desorbed from the coal pore structure earlier. This is consistent with the experimental results [30]. The diffusion rate of O_2 was greater, that is, CO_2 was more easily adsorbed in the coal. With the increase in temperature, the gas molecules at the gas outlet port continued to increase at the same time, indicating that the increase in temperature was conducive to the diffusion of gas in the coal pore structure. From the perspective of the proportion of gas at the outlet port of the pore model at 7500 ps at different temperatures, it can be seen that with the increase in temperature, the proportion of O_2 continued to decrease, indicating that temperature had a greater impact on the adsorption of CO_2 in coal pores.

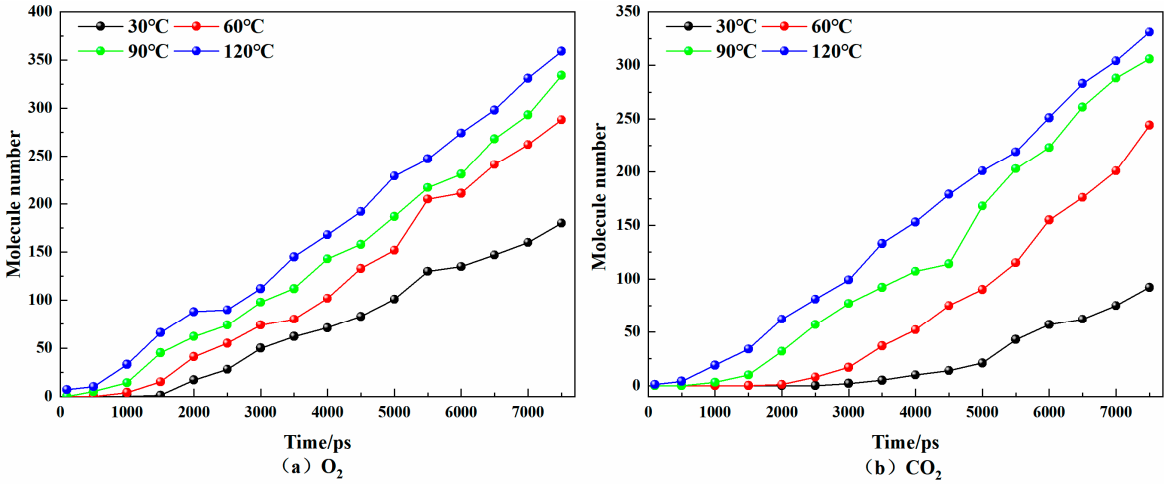

Figure 5. Variations of O_2 and CO_2 with time at the gas outlet port of the coal surface pore model at different temperatures.

Based on gas density profile, the pore space was split into three zones. In order to observe the microscopic mechanism of CO_2 replacing O_2 in pores, taking the pore center of the coal as the center, the number of O_2 and CO_2 molecules in the range of 0~10 Å, 10~15 Å, and 15~20 Å from the center were calculated at a temperature of 30 °C, respectively. The results are shown in Figure 6.

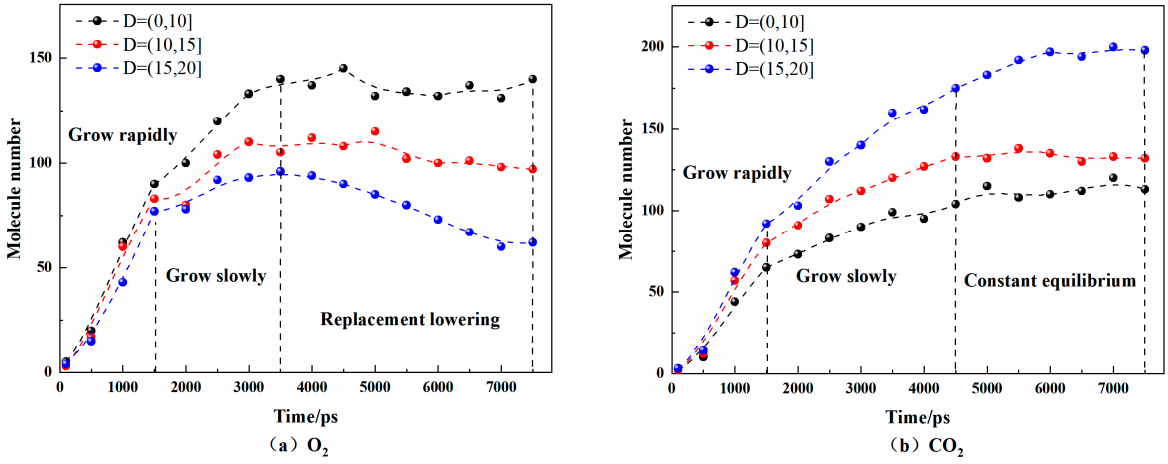

Figure 6. Quantities of O_2 and CO_2 adsorbed in coal pores at 30 °C.

It can be seen that in the whole adsorption process, the number of CO_2 molecules in the pores increased for a longer time than that of O_2. At the same time, the total number CO_2 molecules in the pores was greater, that is, the adsorption capacity of CO_2 was stronger. CO_2 molecules were mainly distributed in the range of 15~20 Å from the center of the pores, and its number in the pores increased rapidly before 1500 ps, then increased slowly from 1500 ps to 4500 ps. After 4500 ps, the numbers in the 0~10 Å and 10~15 Å spatial ranges remained unchanged, while the numbers in the 15~20 Å spatial range increased. O_2 molecules were mainly distributed in the range of 0~10 Å from the center in the coal pores. The O_2 molecules in the pores increased rapidly before 1500 ps, and the growth rate slowed down from 1500 ps to 3500 ps. After 3500 ps, the amount of O_2 in the range of 10~15 Å and 15~20 Å decreased slowly, while the number of CO_2 molecules in the same spatial range increased, indicating that CO_2 replaced O_2 molecules in this space. Additionally, this effect was stronger in the range of 15–20 Å. The number of O_2 and CO_2 molecules fluctuated in the range of 0~10 Å, that is, CO_2 had almost no replacement effect on them.

In a word, in the coal pores, CO_2 tended to be adsorbed more near the pore wall and O_2 tended to be adsorbed in the center of the pores, and the adsorption capacity of coal for CO_2 was stronger than that of O_2. CO_2 could displace the O_2 adsorbed in coal, and this effect was stronger near the pore wall.

3.2. Analysis on the Chemical Mechanism of CO_2 Preventing O_2 Adsorption

3.2.1. Influence of Pre-Injection of CO_2 into Coal on Its Heating Process

From the temperature-programmed experiment, the relationship between the heating rate and the temperature of each coal sample in the oxidation heating process between 30 and 200 °C can be obtained, as shown in Figure 7.

It can be seen from the experimental results that at 124 °C, 50 °C and 120 °C, the heating rates of the AW, YH, and HL coal samples pre-treated with CO_2 injection exceeded that of the coal without CO_2 injection. The above temperatures were in the initial adsorption stage and the fast reaction stage of coal. The turning points of the heating rate curve from rising to falling were all around the slow chemisorption temperature point. Overall, the heating rate of the coal samples injected with CO_2 was lower than that of the coal samples without CO_2 injection (except for YH coal) before the slow chemisorption temperature point. At 170 °C, 120 °C and 141 °C, the temperatures of the AW, YH, and HL coal samples injected with CO_2 exceeded that of the coal without CO_2 injection, and these temperatures were all in the fast reaction stage.

Before the rapid reaction stage, with the increase in coal temperature, the CO_2 adsorbed in the coal sample was gradually desorbed, and O_2 was adsorbed and participated in the reaction to release heat. The slower heating rate of the CO_2-injected coal samples was because the desorbed CO_2 absorbed heat. Moreover, because more CO_2 in coal occupied the adsorption site of O_2, less O_2 was adsorbed during the reaction, which slowed down the oxidation reaction process, so the heat release was slower. After reaching the slow chemisorption temperature point, the coal lost the protective effect of CO_2 due to a large amount of CO_2 extraction. In the early stage, due to the inserting effect of CO_2, the consumption of active groups in the coal was slow. At this time, a large number of active groups combined with O_2 to react, releasing a lot of heat, so the heating rate was faster. The heating rate decreased when the number of active groups decreased. CO_2 was mainly adsorbed in the micropores of coal, and the gas in the micropores was not easily desorbed. The proportion of mesopores in YH coal was larger than that of micropores, while the opposite was true for the AW coal samples and HL coal samples. Therefore, the temperature at which the YH coal sample lost the protective effect of CO_2 was earlier.

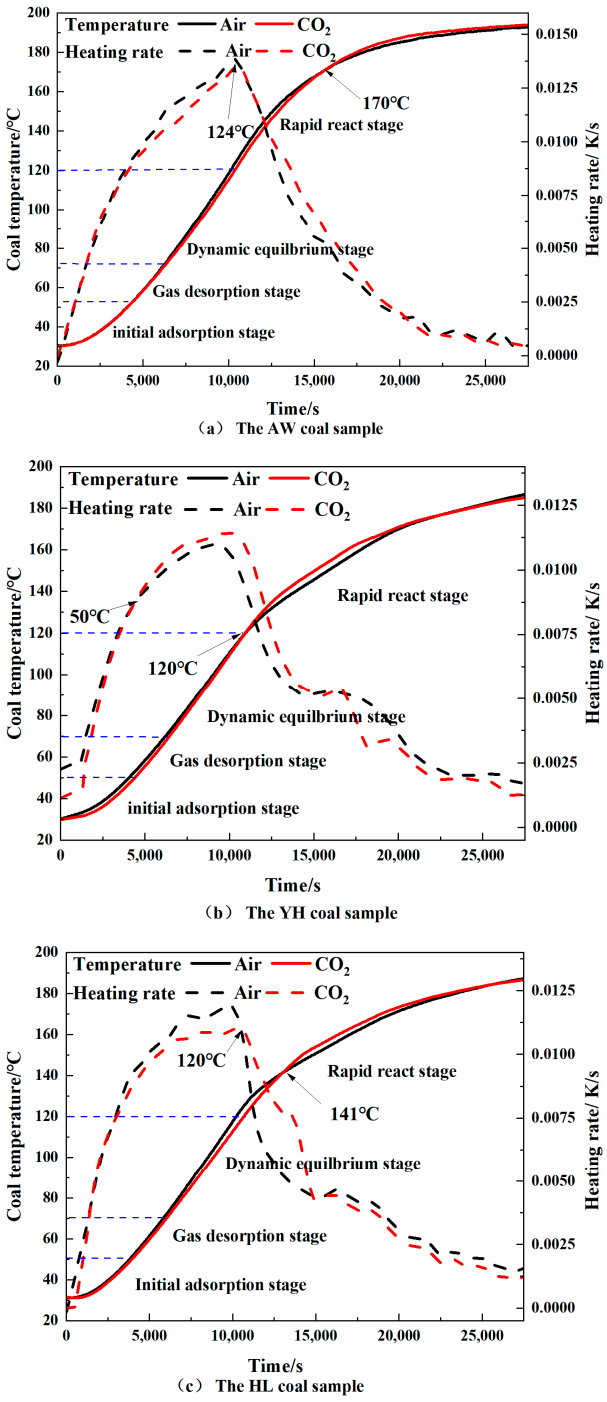

Figure 7. Variation of temperature and heating rate of each coal sample with time.

The Arrhenius formula is often introduced in the analysis of coal oxidation kinetics, and its expression is shown in Formula (1). The Arrhenius formula is based on the elementary reactions of substances and characterizes the relationship between the reaction rate constant and the apparent activation energy.

$$\mathrm{k} = A \exp\left(-\frac{E}{RT}\right) \tag{1}$$

where k is the reaction rate constant (dimensionless); A is the exponent factor (s^{-1}); E is the activation energy (kJ/mol); R is the gas state constant.

Assuming that there is no heat convection, heat conduction, or moisture evaporation during the adiabatic oxidation process of the coal sample, Equation (1) can be transformed into:

$$\ln\left(\frac{dT}{dt}\right) = \ln\left(\frac{Q_c A}{C_c}\right) - \frac{E}{RT} \tag{2}$$

where dT/dt is the heating rate of the adiabatic oxidation of coal, and its value is approximately equal to $(T_1 - T_2)/(t_1 - t_2)$. Using this formula, the apparent activation energy of the experimental coal sample can be obtained.

The relationship between the heating rate of coal and the reciprocal temperature is obtained by Formula (2). It is divided into four stages according to the characteristics of the adsorption and consumption of oxygen, and the fitted straight line of each stage is obtained by linear fitting. The activation energy of coal in each stage of the low-temperature oxidation process is calculated as shown in Figures 8–10.

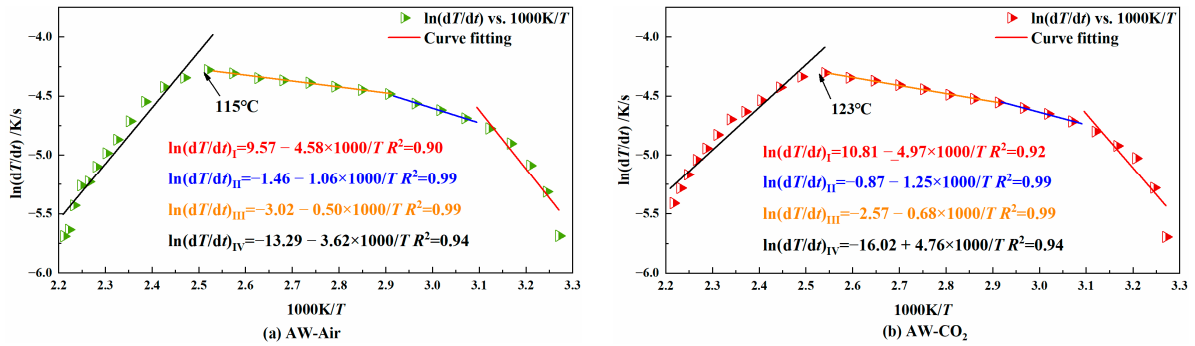

Figure 8. Diagram of the relationship between ln(dT/dt) vs. 1000/T for AW coal sample.

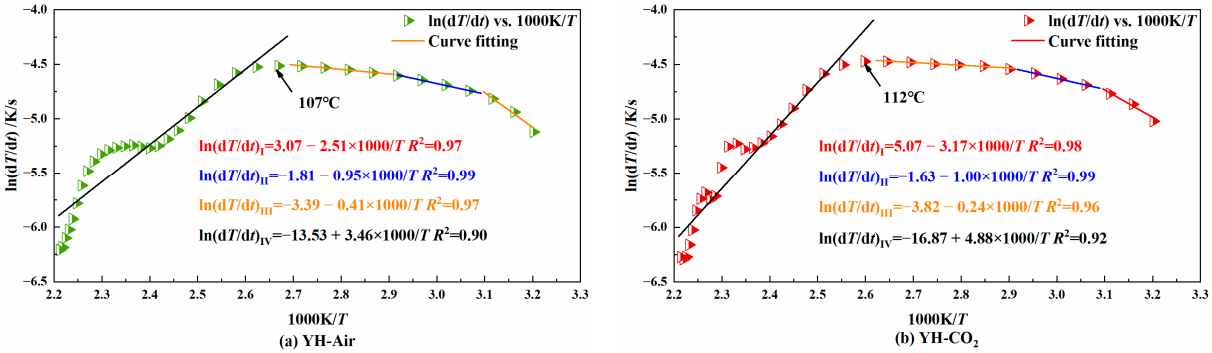

Figure 9. Diagram of the relationship between ln(dT/dt) vs. 1000/T for YH coal sample.

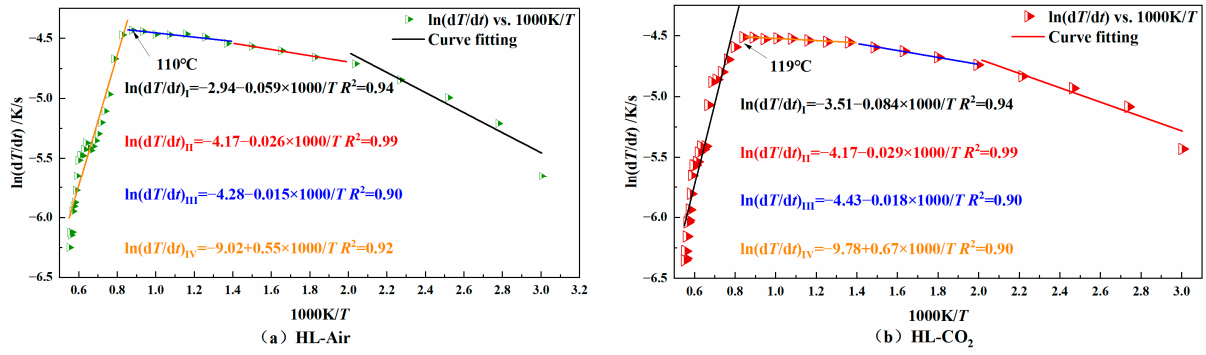

Figure 10. Diagram of the relationship between ln(dT/dt) vs. 1000/T for HL coal sample.

When the slope of the fitted line is negative, it indicates that the coal is in the slow heating stage in the early stage of low-temperature oxidation; when the slope is positive, it indicates that the coal has entered the stage of autothermal oxidation. The temperature corresponding to the turning point where the slope changes from negative to positive is the critical temperature of autoignition. It can be seen from the figure that the whole process of temperature programming can be divided into four stages. From stage I to stage III, the coal is mainly in the early and slow heating process, and stage IV is the autothermal oxidation stage. Table 2 shows the activation energy of each coal sample at each stage.

Table 2. Comparison of activation energy and critical temperature at each stage for the three coal samples with and without CO_2 injection.

Coal Sample	Oxidation Stage	Inject Air		Inject CO_2	
		Activation Energy E_a/kJ/mol	Critical Temperature of Spontaneous Combustion T/°C	Activation Energy E_a/kJ/mol	Critical Temperature of Spontaneous Combustion T/°C
AW	I	38.08	115	41.32	123
	II	8.81		10.39	
	III	4.16		5.65	
	IV	−30.10		−39.58	
YH	I	20.87	107	26.36	112
	II	7.90		8.32	
	III	3.41		2.00	
	IV	−28.77		−40.57	
HL	I	33.67	110	47.72	119
	II	6.90		7.40	
	III	1.08		2.25	
	IV	−34.67		−43.90	

It can be seen from Table 2 that in both stage I and stage II, for the same coal type, the activation energy of the coal injected with CO_2 was higher than that of the coal without CO_2 injection. This shows that the injected CO_2 could hinder the coal's adsorption of O_2 in both stages. In stage III, the activation energy of the CO_2-injected YH coal was lower than that of the non-injected coal, while the opposite was true for the other two coal samples. As already known, this was because the YH coal sample lost the CO_2 adsorption resistance to oxygen at 50 °C. In stage IV, the activation energy of the coal injected with CO_2 was lower than that of the coal not injected with CO_2, indicating that CO_2 lost the effect of oxygen barrier adsorption at about 120 °C.

At about 120 °C, the oxidation process transitioned from stage III to stage IV, and each coal sample reached the critical temperature of spontaneous coal combustion. Additionally, for the same type of coal, the critical temperature of the spontaneous combustion of the coal injected with CO_2 was higher than that of the coal without CO_2 injection, which further showed that the adsorption of CO_2 in the coal had the added effect of preventing oxygen adsorption.

From the above analysis, it can be concluded that the injection of CO_2 into the coal can hinder the O_2 adsorption of its low-temperature oxidation process. Its hindering effect was mainly seen in stage I to stage III, which was manifested as increasing the activation energy of low-temperature coal oxidation and reducing the heating rate of coal. As the temperature increased, CO_2 was desorbed from the coal. Due to the adsorption of CO_2 in the early stage, the consumption of active groups was small. At this time, the active groups adsorbed O_2 in large quantities and reacted, resulting in the intensified low-temperature oxidation of coal. At the same time, the activation energy decreased and the heating rate increased. That is, at stage IV, the coal lost the protective effect of CO_2.

3.2.2. Analysis of Functional Group Changes in CO_2 Injection during Coal Cooling

The in situ infrared experiments obtained the temperature change of the main functional groups of each coal sample under different atmospheric conditions, as shown in Figures 11–16.

(1) Peroxide (C–O–O·)

As shown in Figure 11, in the air atmosphere, the peroxides of the AW and HL coal samples showed a trend of first decreasing and then increasing, but the change range was different. The decrease in the AW coal samples was larger, while the increase in the HL coal samples was larger. The YH coal sample mainly exhibited an increasing trend. The main reason is that during the cooling process in the air atmosphere, the coal sample will chemically adsorb oxygen that is then autocatalyzed into peroxides, but when the temperature is further lowered, the chemical adsorption of oxygen will not be catalyzed into oxides, resulting in an increase in its content. The YH coal sample had a larger proportion of mesopores, so the O_2 adsorption was more rapid, and the peroxide content increased. This was consistent with the above result that the critical temperature of the spontaneous combustion of YH coal was the lowest.

In the CO_2 atmosphere, the absorbance of the peroxides of the AW and HL coal samples first decreased and then increased, and the change range was smaller than that in the air atmosphere. In the YH coal sample, there was a downward trend. This showed that the reaction and generation of peroxides did not change much under anoxic conditions, mainly relying on the partial autocatalytic reaction in the pyrolysis process.

(2) Free hydroxyl (HO·)

The change process of free hydroxyl (HO·) is shown in Figure 12. In the air atmosphere, for the AW coal sample, it first decreased and then tended to be smooth, and in the YH coal sample, it first increased and then tended to be smooth. However, in the HL coal samples, it first decreased and then increased. The free hydroxyl group is the product after peroxide autocatalysis, so it was found that the change trend of the absorbance of the free hydroxyl group and peroxide was similar in the air atmosphere. In the CO_2 atmosphere, the absorbance of free hydroxyl groups in each coal sample first increased and then tended to be smooth, which was similar to the change trend of the peroxide absorbance in the CO_2 atmosphere.

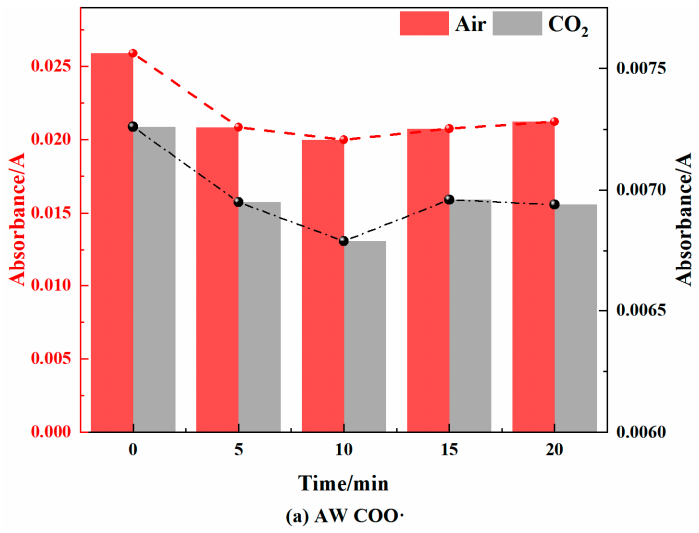

Figure 11. *Cont.*

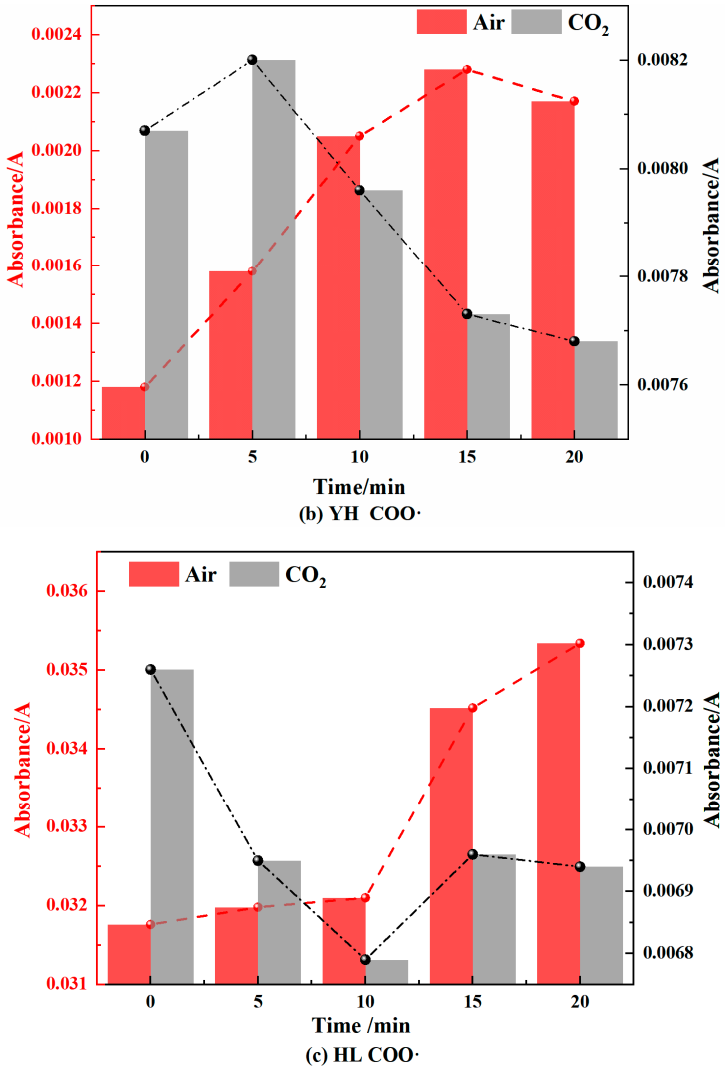

Figure 11. Peroxide Changes in Coal during Cooling Process in Air and CO_2 Atmospheres.

(3) Aldehyde group (-CH=O)

As shown in Figure 13, in the air atmosphere, the aldehyde groups in the AW and YH coal samples first increased and then tended to be smooth, and in the HL coal samples, they showed a trend of first decreasing and then increasing. The aldehyde group is an intermediate product of the coal chemisorption oxygen reaction, which is related to the difference in coal oxidation characteristics. Compared with the AW and YH coal samples, the HL coal samples had more aliphatic side chains, which easily reacted to generate CO or carboxyl groups. In the CO_2 atmosphere, the aldehyde group first increased and then decreased in the AW coal sample, gradually increased in the YH coal sample, and gradually decreased first and then increased in the HL coal sample, but the overall change range was not high. This indicated that a small number of aldehyde group generation and decomposition reactions occurred, and further indicated that the molecular structure of coal changed little during the cooling process under CO_2 atmosphere.

(4) Carboxyl (-COOH)

As shown in Figure 14, in the air atmosphere, the carboxyl groups first decreased and then tended to be smooth in the AW coal sample, first smoothed and then increased in the YH coal sample, and showed an increasing trend in the HL coal sample. This showed that during the cooling process, the carboxyl group of the AW coal sample was generated and the decomposition reaction also occurred. When the temperature decreased,

the decomposition reaction weakened, while the YH coal samples and the HL coal samples were continuously oxidized to form carboxyl groups. In the CO_2 atmosphere, the carboxyl group first increased and then decreased in the AW coal sample, gradually increased in the YH coal sample, and gradually decreased first and then increased in the HL coal sample, but the overall change range was not high. This was the same as for carbonyl changes. It shows that in the CO_2 atmosphere, most carbonyl groups were converted into carboxyl groups, but due to the lack of O_2 in the environment, the main method of generating carboxyl groups was the combination of free hydroxyl groups and carbonyl radicals.

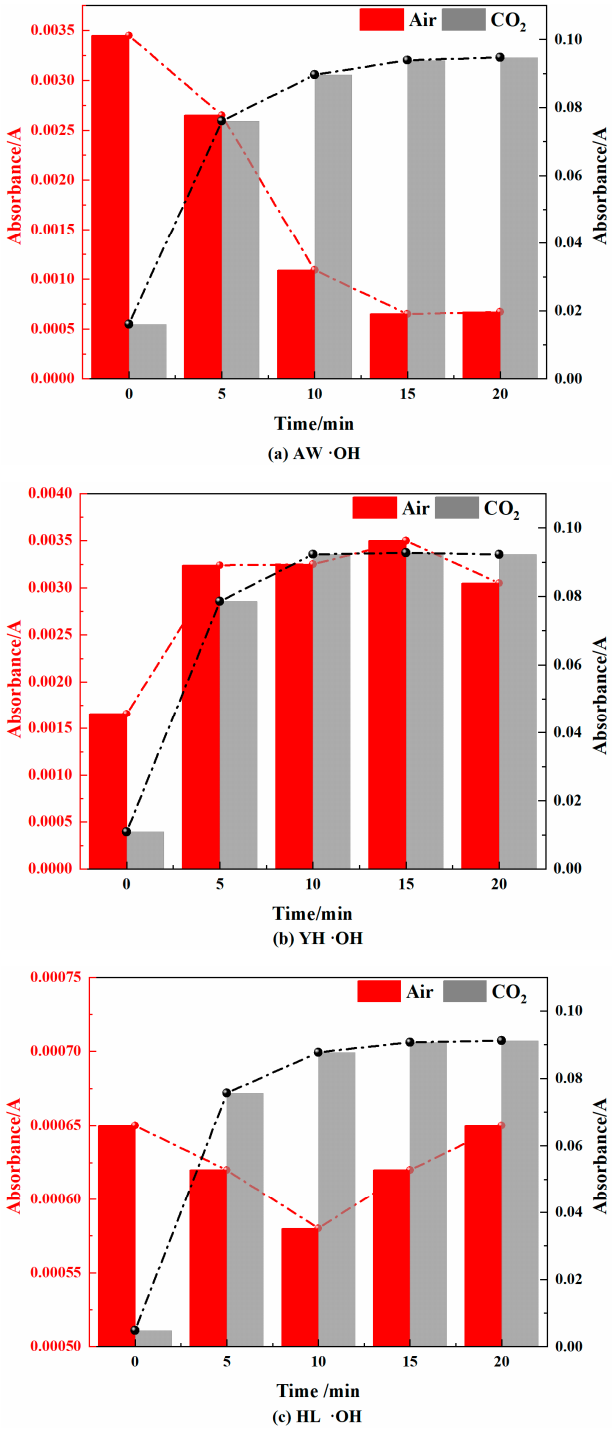

Figure 12. Free Hydroxyl Changes in Coal during Cooling Process in Air and CO_2 Atmospheres.

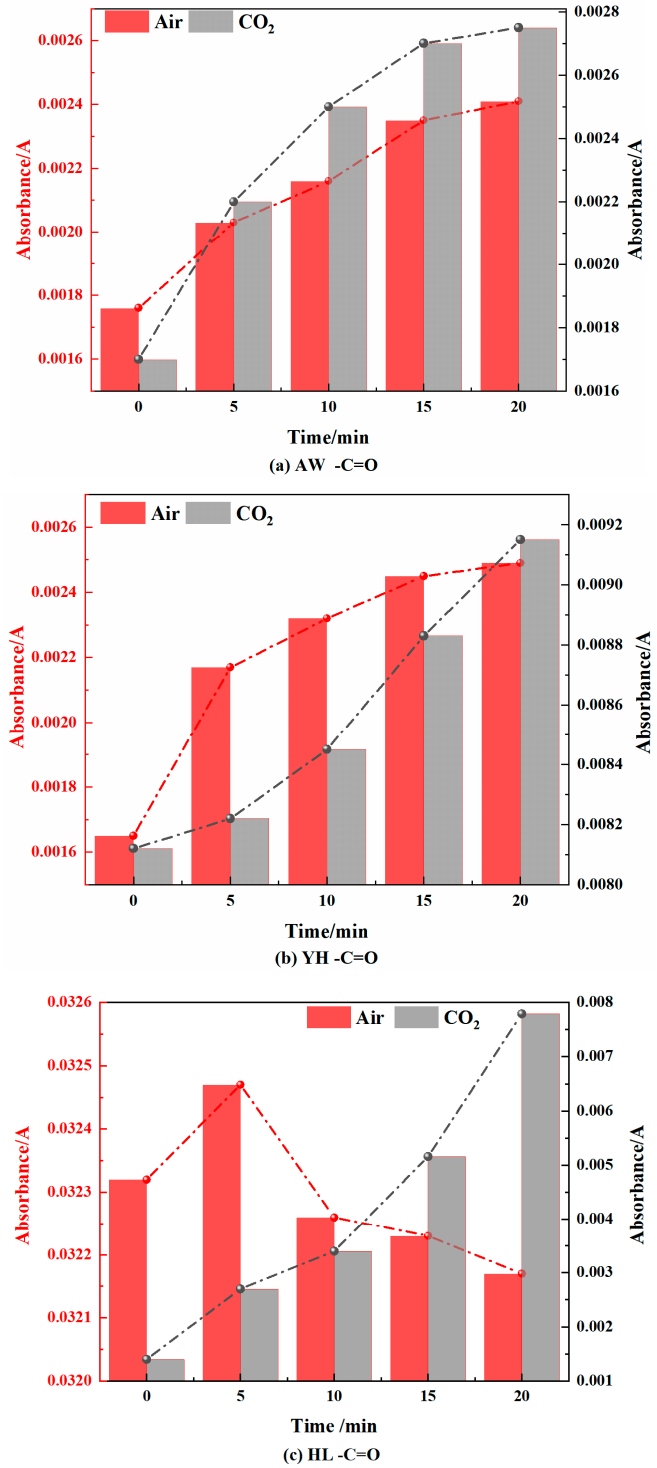

Figure 13. Carbonyl Changes in Coal during Cooling Process in Air and CO_2 Atmospheres.

(5) Methyl ($-CH_3$) and methylene ($-CH_2-$)

It can be seen from Figures 14 and 15 that in the air atmosphere, the methyl group and the methylene group showed a trend of increasing first and then decreasing. The main reason is that pyrolysis breaks aliphatic chains in coal to generate methyl and methylene groups. They then interact with oxygen for chemisorption reactions and low-temperature condensation.

In the CO_2 atmosphere, the absorbance of methyl and methylene increased first and then decreased, which was caused by the pyrolysis reaction and the condensation

of aliphatic chains. In an oxygen-deficient environment, the aliphatic chain of the coal molecule is broken to form methyl and methylene at high temperatures, which are condensed at low temperatures. However, the changes in methyl and methylene in the air atmosphere were not as large as those in the CO_2 atmosphere.

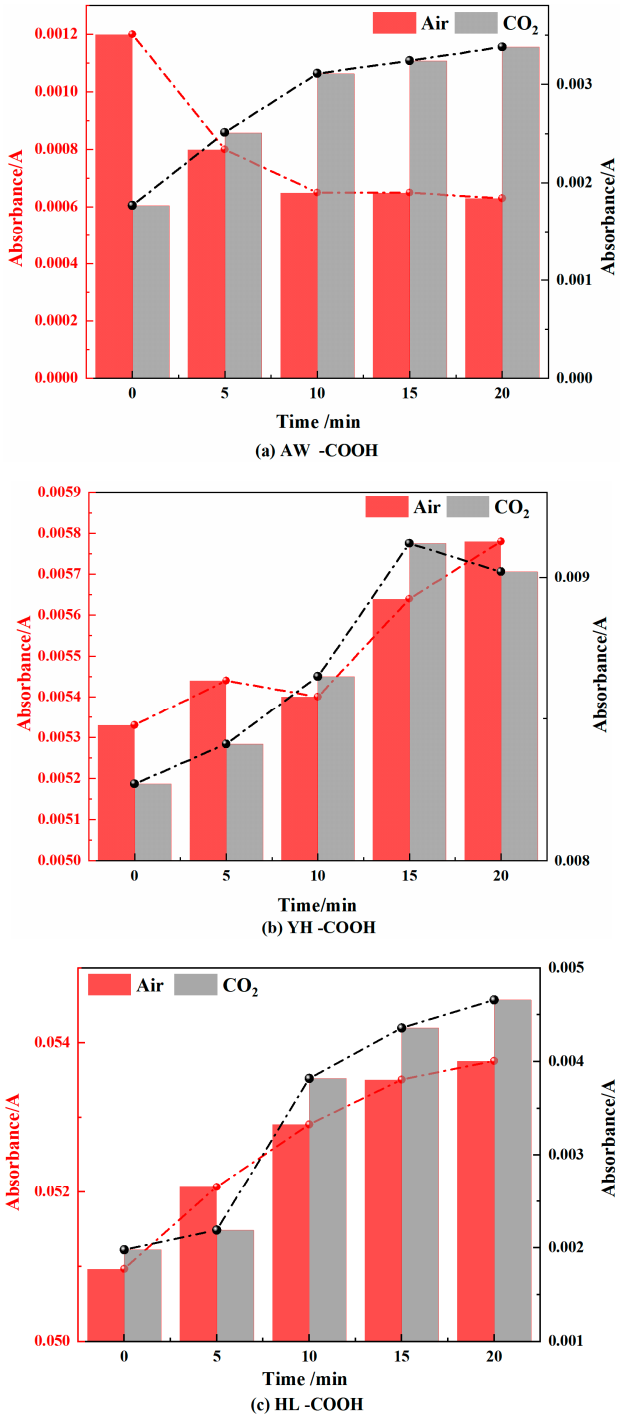

Figure 14. Carboxyl Changes in Coal during Cooling Process in Air and CO_2 Atmospheres.

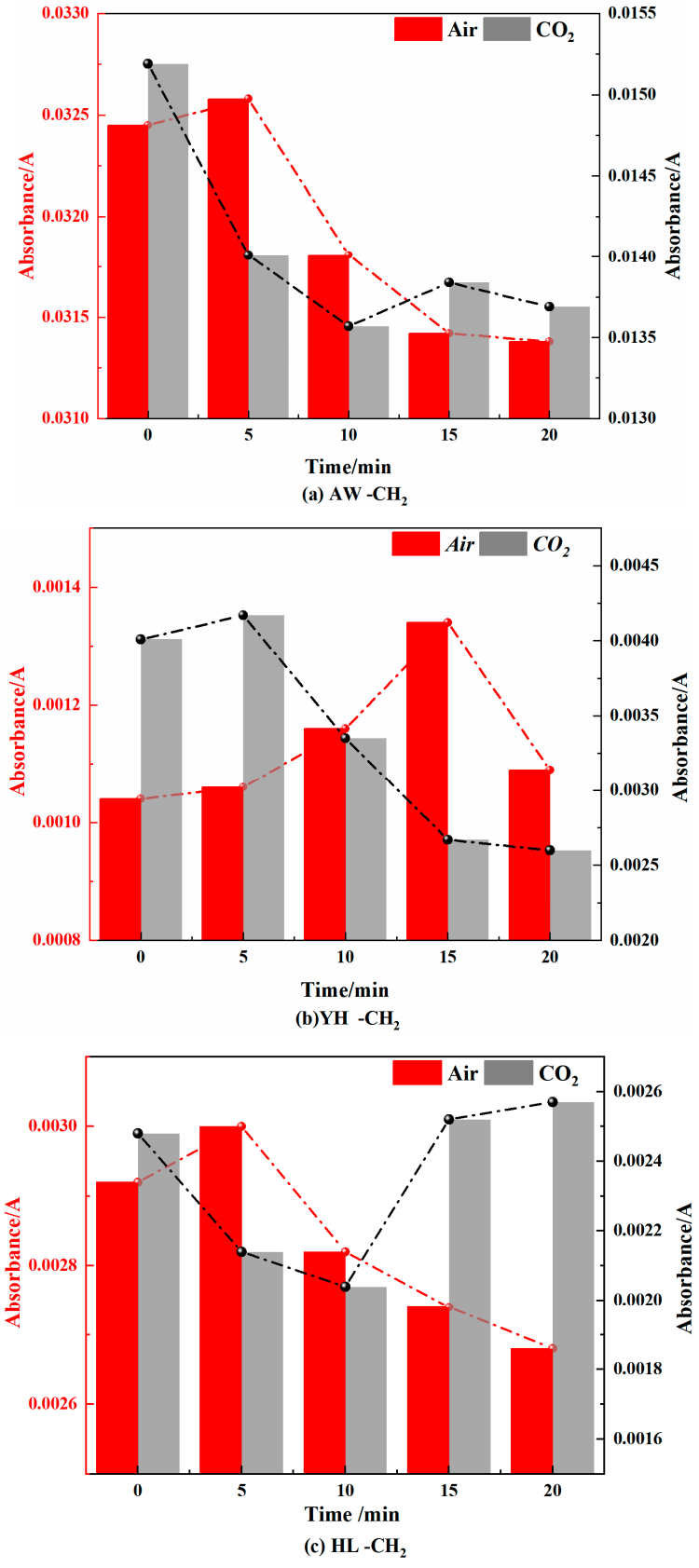

Figure 15. Methylene Changes in Coal during Cooling Process in Air and CO_2 Atmospheres.

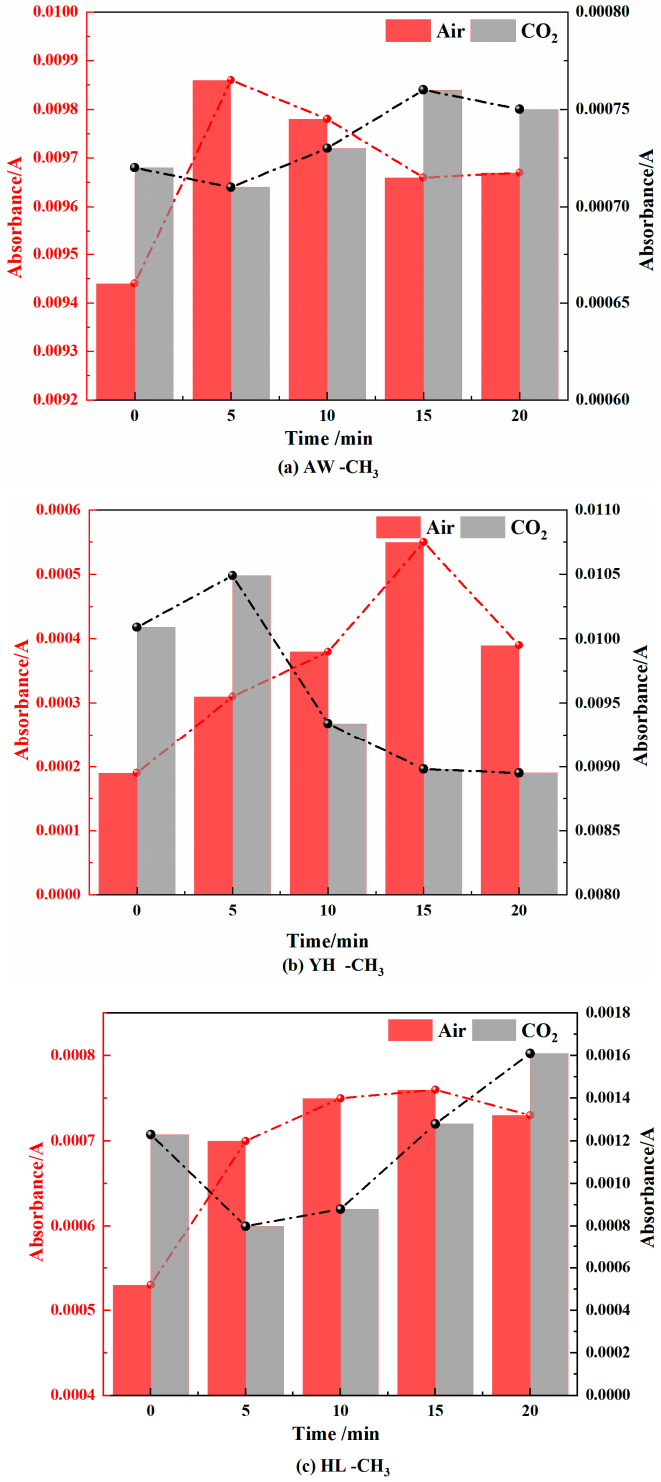

Figure 16. Methyl Changes in Coal during Cooling Process in Air and CO_2 Atmospheres.

Through the above analysis, it can be concluded that when the coal was cooled in the air atmosphere, the chemisorption products of coal oxide such as ·OH and C-O-O·, -CH=O and -COOH increased. When the coal was cooled in the CO_2 atmosphere, the main pyrolysis and condensation reactions occurred due to the lack of O_2, and CO_2 hindered the decomposition of -COOH, etc., which eventually led to the increase in -CH=O and -COOH in the coal. Other structural changes were smaller.

3.2.3. Effect of CO_2 on the Reaction Process of Coal Chemical Adsorption of O_2

While hindering the adsorption of O_2 by coal, CO_2 will have a weak interaction with coal molecules and O_2 molecules, which will affect the activation energy and exothermic conditions of the reaction process of the chemical adsorption of oxygen by coal, thereby affecting the reaction process. Taking methyl as an example, the chemical adsorption reaction process of coal was constructed as follows [28]:

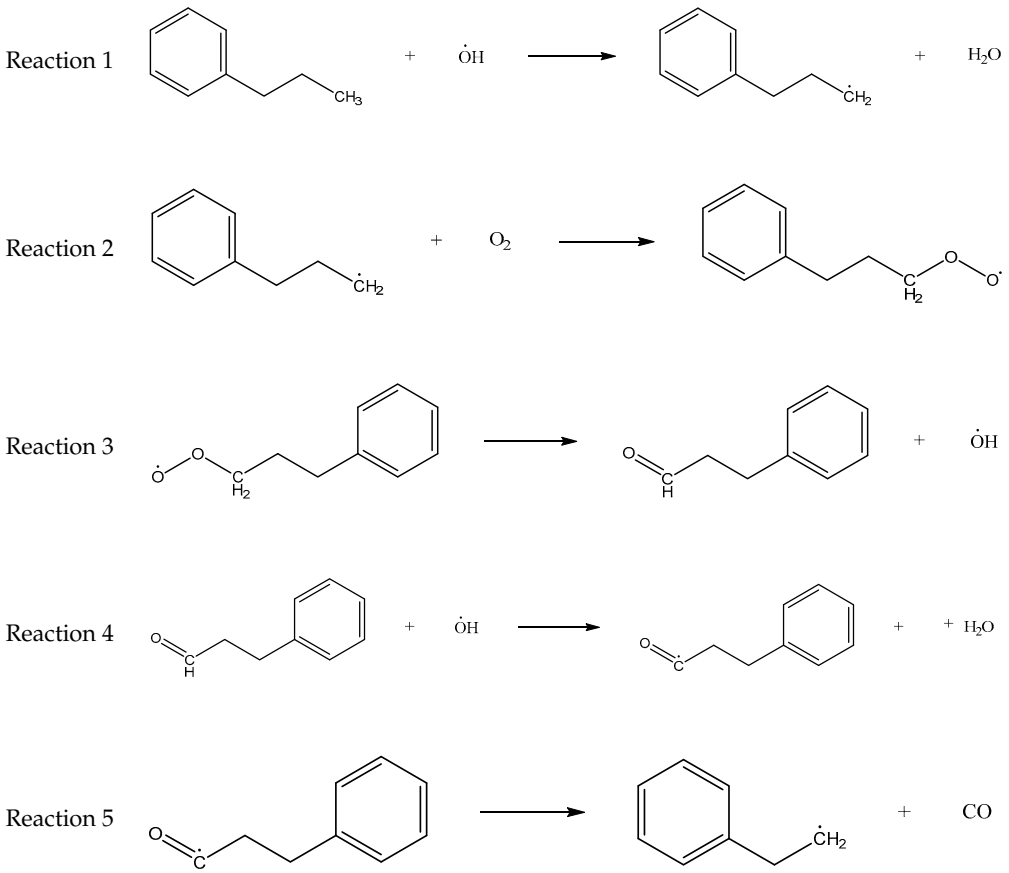

The above reactions were simulated with and without CO_2, respectively. CO_2 had little effect on the activation energy of reaction 1, but had a significant effect on its heat release. When CO_2 was present, the heat release increased from 54.07 kJ/mol to 59.19 kJ/mol. Reaction 2 is the chemisorption of O_2, which does not require activation energy, and its exothermic heat was reduced from 141.49 kJ/mol to 125.37 kJ/mol in the presence of CO_2. Reaction 3 involves the active group in the chemisorbed state abstracting the surrounding hydrogen atoms. The presence of CO_2 reduced the activation energy of the reaction from 66.98 kJ/mol to 60.34 kJ/mol, and at the same time increased the heat release from 103.14 kJ/mol to 110.39 kJ/mol. The presence of CO_2 had little effect on the activation energy of reaction 4, but it could reduce the heat release from 99.73 kJ/mol to 90.22 kJ/mol. The effect of CO_2 on the activation energy and heat change of reaction 5 was more prominent: the activation energy increased from 48.55 kJ/mol to 61.49 kJ/mol and the heat absorption increased from 26.29 kJ/mol to 49.21 kJ/mol. The detailed heat change is shown in Figure 17.

To sum up, CO_2 had no significant effect on reaction 1 or reaction 4, it reduced the exothermic heat of reaction 2, thereby affecting the subsequent reaction process, and it promoted reaction 3 and hindered reaction 5.

It can be seen from the above that the injection of CO_2 will increase the carboxyl and aldehyde groups in the coal. According to the simulation results, this can be explained by CO_2 having a weak effect on the reaction of hydroxyl radicals and hindering the generation

of CO, thus reducing the consumption of the above functional groups. CO_2 hinders the chemical adsorption reaction between O_2 and coal surface molecules, resulting in the inability of the continuous generation of hydroxyl radicals, thus playing a role in chemical inhibition. On the whole, CO_2 has an inhibitory effect on the reaction of coal chemical adsorption of O_2.

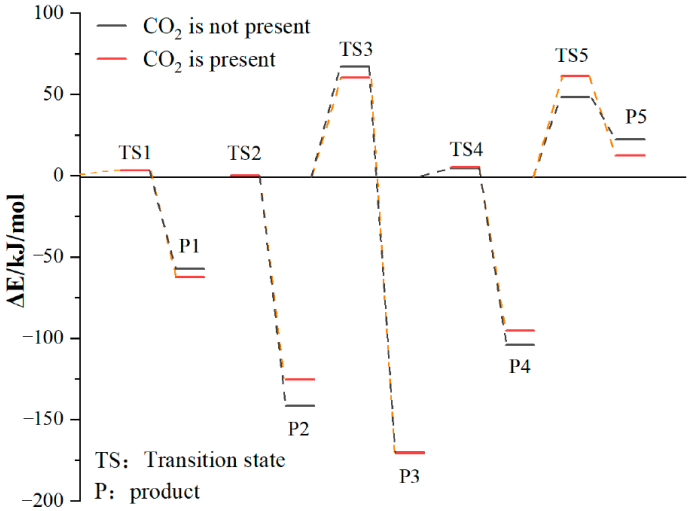

Figure 17. Changes in reaction energy in the absence and presence of CO_2.

3.3. Construction of the Model of CO_2 Prevents O_2 Adsorption

It can be seen from the above that CO_2 inhibited oxygen adsorption during the low-temperature oxidation of coal, and this effect included physical inhibition and chemical inhibition. Additionally, according to the experimental results and molecular simulation results, it was found that the effect of CO_2 on preventing O_2 adsorption was also different in the different stages of low-temperature coal oxidation. Therefore, the model of CO_2 physical–chemical inhibition of O_2 adsorption was established as shown in Figure 18.

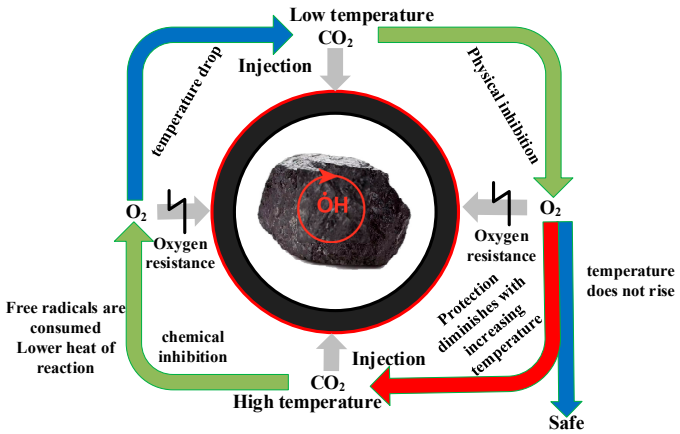

Figure 18. The model of CO_2 physical–chemical prevention of O_2 adsorption.

At low temperatures, injecting CO_2 into the coal can form a protective layer on the surface of the coal, thereby blocking the contact between the coal and O_2, and achieving the effect of inhibiting the low-temperature oxidation of the coal. At the same time, it can also replace the O_2 adsorbed on the coal surface, resulting in physical inhibition. However, it was found through experiments that when the temperature rose to the point of slow chemical adsorption, CO_2 lost its protective effect on the coal surface, and the coal and O_2 produced low-temperature oxidation after interacting again, resulting in an increase in the heating rate of coal. When coal temperature rises, a chemical adsorption chain reaction

is formed inside the coal. The injection of CO_2 at a high temperature will dilute the O_2 concentration in the coal, thereby reducing the chemical adsorption reaction between coal and O_2, and at the same time increasing the activation energy and reducing the reaction heat. This creates a chemical inhibition. At the same time, due to the reduction of the coal chemical adsorption oxygen reaction, the free radicals cannot be generated and are continuously consumed, which slows down the low-temperature oxidation reaction process of coal and reduces the heat release. This achieves the effect of preventing the reaction from occurring.

4. Conclusions

(1) The adsorption capacity of coal pores for CO_2 is stronger than that of O_2. CO_2 tends to be adsorbed near the pore wall and O_2 tends to be adsorbed in the center of the pores. Moreover, CO_2 can replace O_2 adsorbed in coal, and the replacement mostly occurs in the area near the pore wall.

(2) The injection of CO_2 can block the adsorption of O_2 in the low-temperature oxidation process of coal, its hindering effect is mainly exerted in the slow heating stage, and at about 120 °C, the coal loses the protective effect of CO_2.

(3) When coal is cooled in a CO_2 atmosphere, the coal will mainly undergo pyrolysis and condensation reactions, which eventually leads to the increase in -CH=O and -COOH in the coal, and the changes in other structures are small.

(4) In the chemisorption chain reaction of coal oxide, the effect of CO_2 on each step of the reaction chain is not the same, but in general, it increases the activation energy and reduces the heat release, which has the effect of inhibiting the chemical reaction.

(5) In this paper, the model of carbon dioxide physical–chemical oxygen barrier adsorption is constructed based on experiments and simulations, which lacks field practice verification. However, the research in this paper can guide the work and improve the efficiency of underground fire prevention in coal mines and save labor, time, and material resources.

Author Contributions: G.C. writing original draft, experiments and simulation methods and data arrangement; H.W. provide coal sample and editing. B.T. writing review; S.F. simulating that the coal adsorbs oxygen. All authors have read and agreed to the published version of the manuscript.

Funding: This research was supported by the National Natural Science Foundation of China (52074156, 51804355, 51864045, 51774291), the Fundamental Research Funds for the Central Universities (2022YJSAQ13), Introduction Plan for "Tianchi Talent" in Xinjiang Uygur Autonomous Region.

Institutional Review Board Statement: Not applicable.

Informed Consent Statement: Not applicable.

Data Availability Statement: Not applicable.

Conflicts of Interest: The authors declare no conflict of interest.

References

1. Song, Z.; Kuenzer, C.; Zhu, H.; Zhang, Z.; Jia, Y.; Sun, Y.; Zhang, J. Analysis of coal fire dynamics in the Wuda syncline impacted by fire-fighting activities based on in-situ observations and Landsat-8 remote sensing data. *Int. J. Coal. Geol.* **2015**, *141–142*, 91–102. [CrossRef]
2. Liu, J.; Wang, Y.; Yan, S.; Zhao, F.; Li, Y.; Dang, L.; Liu, X.; Shao, Y.; Peng, B. Underground Coal Fire Detection and Monitoring Based on Landsat-8 and Sentinel-1 Data Sets in Miquan Fire Area, XinJiang. *Remote Sens.* **2021**, *13*, 1141. [CrossRef]
3. Tan, B.; Zhang, F.; Zhang, Q.; Wei, H.; Shao, Z. Firefighting of subsurface coal fires with comprehensive techniques for detection and control: A case study of the Fukang coal fire in the Xinjiang region of China. *Environ. Sci. Pollut. Res.* **2019**, *26*, 29570–29584. [CrossRef] [PubMed]
4. Wang, T.; Wang, Y.; Zhao, F.; Feng, H.; Liu, J.; Zhang, L.; Zhang, N.; Yuan, G.; Wang, D. A spatio-temporal temperature-based thresholding algorithm for underground coal fire detection with satellite thermal infrared and radar remote sensing. *Int. J. Appl. Earth Obs. Geoinf.* **2022**, *110*, 102805. [CrossRef]

5. Song, Z.; Kuenzer, C. Coal fires in China over the last decade: A comprehensive review. *Int. J. Coal. Geol.* **2014**, *133*, 72–99. [CrossRef]
6. Shao, Z.; Jia, X.; Zhong, X.; Wang, D.; Wei, J.; Wang, Y.; Chen, L. Detection, extinguishing, and monitoring of a coal fire in Xinjiang, China. *Environ. Sci. Pollut. Res.* **2018**, *25*, 26603–26616. [CrossRef] [PubMed]
7. Wang, Y.; Ge, S.; Guo, G. (Eds.) *Mining Science and Technology: Proceedings of the 5th International Symposium on Mining Science and Technology, Xuzhou, China, 20–22 October 2004*; CRC Press: Boca Raton, FL, USA, 2004.
8. Wang, H.; Dlugogorski, B.; Kennedy, E. Kinetic modeling of low-temperature oxidation of coal. *Combust. Flame* **2002**, *131*, 452–464. [CrossRef]
9. Tan, B.; Cheng, G.; Zhu, X.; Yang, X. Experimental Study on the Physisorption Characteristics of O_2 in Coal Powder are Effected by Coal Nanopore Structure. *Sci. Rep.* **2020**, *10*, 6946. [CrossRef]
10. Karsner, G.G.; Perlmutter, D.D. Model for coal oxidation kinetics. 1. Reaction under chemical control. *Fuel* **1982**, *61*, 29–34. [CrossRef]
11. Wang, H.; Dlugogorski, B.Z.; Kennedy, E.M. Coal oxidation at low temperatures: Oxygen consumption, oxidation products, reaction mechanism and kinetic modelling. *Prog. Energy Combust. Sci.* **2003**, *29*, 487–513. [CrossRef]
12. Xue, D.; Hu, X.; Cheng, W.; Wu, M.; Shao, Z.; Li, Y.; Zhao, Y.; Zhang, K. Carbon dioxide sealing-based inhibition of coal spontaneous combustion: A temperature-sensitive micro-encapsulated fire-retardant foamed gel. *Fuel* **2020**, *266*, 117036. [CrossRef]
13. Liu, Y.; Wen, H.; Guo, J.; Jin, Y.; Wei, G.; Yang, Z. Coal spontaneous combustion and N_2 suppression in triple goafs: A numerical simulation and experimental study. *Fuel* **2020**, *271*, 117625. [CrossRef]
14. Zhang, Y.; Xu, J.; Wang, D. Experimental Study on the Inhibition Effects of Nitrogen and Carbon Dioxide on Coal Spontaneous Combustion. *Energies* **2020**, *13*, 5256. [CrossRef]
15. Deng, J.; Ren, L.F.; Ma, L.; Qin, X.Y.; Wang, W.F.; Liu, C.C. Low-temperature oxidation and reactivity of coal in O_2/N_2 and O_2/CO_2 atmospheres, a case of carboniferous–permian coal in Shaanxi, China. *Environ. Earth Sci.* **2019**, *78*, 234. [CrossRef]
16. Khatami, R.; Stivers, C.; Levendis, Y.A. Ignition characteristics of single coal particles from three different ranks in O_2/N_2 and O_2/CO_2 atmospheres. *Combust. Flame* **2012**, *159*, 3554–3568. [CrossRef]
17. Wang, F.; Liu, H.W. Comparative experiment study on fire prevention and extinguishing in goaf by N-$_2$-water mist and CO_2-water mist. *Arab. J. Geosci.* **2020**, *13*, 856. [CrossRef]
18. Liu, W.; Chu, X.; Xu, H.; Chen, W.; Ma, L.; Qin, Y.; Wei, J. Oxidation reaction constants for coal spontaneous combustion under inert gas environments: An experimental investigation. *Energy* **2022**, *247*, 123457. [CrossRef]
19. Su, H.; Kang, N.; Shi, B.; Ji, H.; Li, Y.; Shi, J. Simultaneous thermal analysis on the dynamical oxygen-lean combustion behaviors of coal in a O-$_2$/N-$_2$/CO_2 atmosphere. *J. Energy Inst.* **2021**, *96*, 128–139. [CrossRef]
20. Liu, H.W.; Wang, F. Thermal characteristics and kinetic analysis of coal-oxygen reaction under the condition of inert gas. *Int. J. Coal Prep. Util.* **2022**, *42*, 846–862. [CrossRef]
21. Wu, L.; Qiao, Y.; Yao, H. Experimental and numerical study of pulverized bituminous coal ignition characteristics in O_2/N_2 and O_2/CO_2 atmospheres. *Asia-Pac. J. Chem. Eng.* **2012**, *7*, S195–S200. [CrossRef]
22. Li, Q.; Zhao, C.; Chen, X.; Wu, W.; Lin, B. Properties of char particles obtained under O_2/N_2 and O_2/CO_2 combustion environments. *Chem. Eng. Process. Process Intensif.* **2010**, *49*, 449–459. [CrossRef]
23. Ma, L.; Yu, W.; Ren, L.; Qin, X.; Wang, Q. Micro-characteristics of low-temperature coal oxidation in CO_2/O_2 and N_2/O_2 atmospheres. *Fuel* **2019**, *246*, 259–267. [CrossRef]
24. Zhou, B.; Yang, S.; Yang, W.; Jiang, X.; Song, W.; Cai, J.; Xu, Q.; Tang, Z. Variation characteristics of active groups and macroscopic gas products during low-temperature oxidation of coal under the action of inert gases N-$_2$ and CO_2. *Fuel* **2022**, *307*, 121893. [CrossRef]
25. Wu, S.; Jin, Z.; Deng, C. Molecular simulation of coal-fired plant flue gas competitive adsorption and diffusion on coal. *Fuel* **2019**, *239*, 87–96. [CrossRef]
26. Zhang, J.; Wang, J.; Zhang, C.; Li, Z.; Zhu, J.; Lu, B. Molecular simulation of gases competitive adsorption in lignite and analysis of original CO desorption. *Sci. Rep.* **2021**, *11*, 11706. [CrossRef] [PubMed]
27. Long, H.; Lin, H.F.; Yan, M.; Bai, Y.; Tong, X.; Kong, X.G.; Li, S.G. Adsorption and diffusion characteristics of CH_4, CO_2, and N_2 in micropores and mesopores of bituminous coal: Molecular dynamics. *Fuel* **2021**, *292*, 120268. [CrossRef]
28. Dong, X.; Wang, F.; Guo, L.; Zhang, Y.; Dong, X. Investigation of Competitive Adsorption Properties of $CO/CO_2/O_2$ onto the Kailuan Coals by Molecular Simulation. *ACS Omega* **2022**, *7*, 19305–19318. [CrossRef]
29. Liu, Y.; Fu, P.; Bie, K.; Gong, Y.; Xu, T. The intrinsic reactivity of coal char conversion compared under different conditions of O_2/CO_2, O_2/H_2O and air atmospheres. *J. Energy Inst.* **2020**, *93*, 1883–1891. [CrossRef]
30. Liu, M.-X.; Shi, G.-Q.; Guo, Z.; Wang, Y.-M.; Ma, L.-Y. 3-D simulation of gases transport under condition of inert gas injection into goaf. *Heat Mass Transf.* **2016**, *52*, 2723–2734. [CrossRef]
31. Yan, F.; Xu, J.; Peng, S.; Zou, Q.; Zhou, B.; Long, K.; Zhao, Z. Breakdown process and fragmentation characteristics of anthracite subjected to high-voltage electrical pulses treatment. *Fuel* **2020**, *275*, 117926. [CrossRef]
32. Yan, F.; Xu, J.; Lin, B.; Peng, S.; Zou, Q.; Zhang, X. Changes in pore structure and permeability of anthracite coal before and after high-voltage electrical pulses treatment. *Powder Technol.* **2019**, *343*, 560–567. [CrossRef]
33. Ren, J.; Song, Z.; Li, B.; Liu, J.; Lv, R.; Liu, G. Structure feature and evolution mechanism of pores in different metamorphism and deformation coals. *Fuel* **2021**, *283*, 119292. [CrossRef]

34. Kamran, U.; Rhee, K.Y.; Park, S.-J. Effect of Triblock Copolymer on Carbon-Based Boron Nitride Whiskers for Efficient CO_2 Adsorption. *Polymers* **2019**, *11*, 913. [CrossRef] [PubMed]
35. Kamran, U.; Rhee, K.Y.; Lee, S.Y.; Park, S.J. Solvent-free conversion of cucumber peels to N-doped microporous carbons for efficient CO_2 capture performance. *J. Clean. Prod.* **2022**, *369*, 133367. [CrossRef]
36. Kamran, U.; Park, S.J. Acetic acid-mediated cellulose-based carbons: Influence of activation conditions on textural features and carbon dioxide uptakes. *J. Colloid Interface Sci.* **2021**, *594*, 745–758. [CrossRef]
37. Fu, S.; Tan, B.; Cheng, G.; Wang, H.; Fang, X.; Shao, Z.; Li, Z. Study of Adsorption Characteristics of CO_2, O_2, and N_2 in Coal Micropores and Mesopores at Normal Pressure. *Ind. Eng. Chem. Res.* **2022**, *61*, 12845–12856. [CrossRef]
38. Bai, Y.; Lin, H.-F.; Li, S.-G.; Yan, M.; Long, H. Molecular simulation of N_2 and CO_2 injection into a coal model containing adsorbed methane at different temperatures. *Energy* **2021**, *219*, 119686. [CrossRef]
39. Cheng, G.; Tan, B.; Zhang, Z.; Fu, S.; Haiyan, W.; Wang, F. Characteristics of coal-oxygen chemisorption at the low-temperature oxidation stage: DFT and experimental study. *Fuel* **2022**, *315*, 123120. [CrossRef]
40. Zhu, H.; Huo, Y.; Wang, W.; He, X.; Fang, S.; Zhang, Y. Quantum chemical calculation of reaction characteristics of hydroxyl at different positions during coal spontaneous combustion. *Process Saf. Environ. Prot.* **2021**, *148*, 624–635. [CrossRef]
41. Chen, Q.; Zheng, J.; Xu, J.; Dang, Z.; Zhang, L. Insights into sulfamethazine adsorption interfacial interaction mechanism on mesoporous cellulose biochar: Coupling DFT/FOT simulations with experiments. *Chem. Eng. J.* **2019**, *356*, 341–349. [CrossRef]